Electrophoretic Nuclei Assembly for Crystallization of High-Performance Membranes on Unmodified Supports

Guangwei He, Mostapha Dakhchoune, Jing Zhao, Shiqi Huang, and Kumar Varoon Agrawal*

Metal–organic framework (MOF) films have recently emerged as highly permselective membranes yielding orders of magnitude higher gas permeance than that from the conventional membranes. However, synthesis of highly intergrown, ultrathin MOF films on porous supports without complex support-modification has proven to be a challenge. Moreover, there is an urgent need of a generic crystallization route capable of synthesizing a wide range of MOF structures in an intergrown, thin-film morphology. Herein, a novel electrophoretic nuclei assembly for crystallization of highly intergrown thin-films (ENACT) approach, that allows synthesis of ultrathin, defect-free ZIF-8 on a wide range of unmodified supports (porous polyacrylonitrile, anodized aluminum oxide, metal foil, porous carbon and graphene), is reported. As a result, a remarkably high H_2 permeance of 8.3×10^{-6} mol m^{-2} s^{-1} Pa^{-1} and ideal gas selectivities of 7.3, 15.5, 16.2, and 2655 for H_2/CO_2, H_2/N_2, H_2/CH_4, and H_2/C_3H_8, respectively, are achieved from an ultrathin (500 nm thick) ZIF-8 membrane. A high C_3H_6 permeance of 9.9×10^{-8} mol m^{-2} s^{-1} Pa^{-1} and an attractive C_3H_6/C_3H_8 selectivity of 31.6 are obtained. The ENACT approach is straightforward, reproducible and can be extended to a wide range of nanoporous crystals, and its application in the fabrication of intergrown ZIF-7 films is demonstrated.

1. Introduction

Molecular selective films derived from the family of metal–organic frameworks (MOFs) have attracted escalating attention due to their tremendous prospect as membranes, electrocatalysts, batteries, sensors, supercapacitors, etc.[1–4] A large database of MOF structures is available owing to the combinatorial and reticular chemistry of linkers and metal ions.[5] However, only a few MOF structures such as ZIF-7, -8, -9, -11, -67, -90, HKUST-1, MIL-53, and UiO-66 have been fabricated into single-phase membranes, mainly due to the difficulty in controlling heterogeneous nucleation on porous support and subsequent crystal growth.[6–9] Even among these structures, crystallization of ultrathin (<500 nm thick, refer to Section I, Supporting Information), high-performance (high permeance

and selectivity) MOF membranes on porous supports is a challenging task.[10–12] Given that a high heterogeneous nucleation density is required to synthesize an ultrathin, highly intergrown MOF film, development of a generic technique that achieves this goal on a wide range of substrates is highly attractive.

Recently, ZIF-8 membranes have been intensively investigated for H_2/CO_2,[13,14] H_2/CH_4,[15] H_2/C_3H_8,[16,17] and C_3H_8/C_3H_6[18,19] separations (refer to Section II, Supporting Information). Most of the studies have achieved successful synthesis of high-performance ZIF-8 membranes only after modifying the functionality or topography of the underlying porous support. Peinemann and co-workers fabricated an ultrathin ZIF-8 membrane on a metal chelating polythiosemicarbazide (PTSC) support.[16] The chelating ability of the PTSC rendered a high density of zinc ions at the support surface, which facilitated a uniform heterogeneous nucl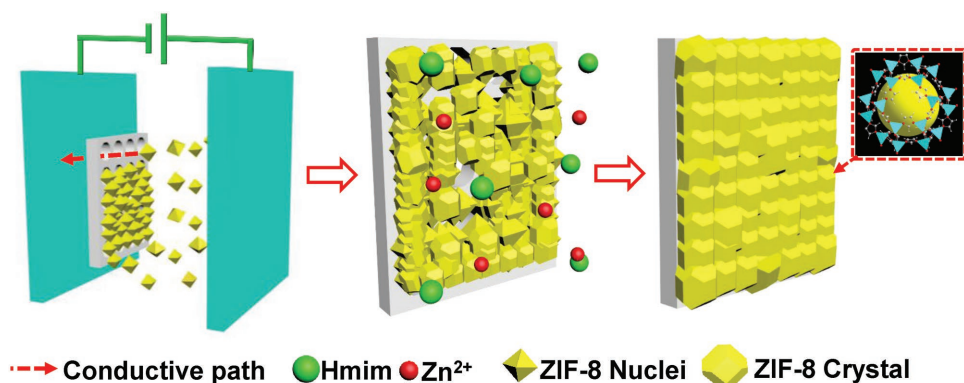eation of ZIF-8 on the polymeric support. Chen and co-workers reported synthesis of 1 µm thick ZIF-8 membranes on (3-aminopropyl)triethoxysilane-functionalized TiO_2-coated polyvinylidene fluoride (PVDF) hollow fibers.[20] Here, the terminal amine groups and nanostructured titania promoted a high nucleation density of ZIF-8 on the PVDF substrate, which is needed for a high grain intergrowth in the film. Wang and co-workers prepared an ultrathin ZIF-8 membrane using graphene oxide/ZIF-8 hybrid nanosheets as seeds.[21] The nanosheets packed well into a dense seeding layer, requiring only a mild intergrowth to seal intersheet gaps. Li et al. reported ultrathin ZIF-8 membranes on ethanediamine-modified PVDF supports by the gel–vapor deposition technique, leading to one of the best separation performances.[22] However, it is highly desirable to synthesize high-performance MOF membranes on supports while avoiding complex surface functionalizations.

Herein, we report a one-step, highly reproducible, and a generic route to synthesize highly intergrown and ultrathin ZIF-8 films on unmodified supports (360 nm thick on porous polyacrylonitrile, PAN, and 500 nm thick on anodic aluminum oxide, AAO), which displayed one of the best gas separation performances ever reported. A remarkably high H_2 permeance of 8.3×10^{-6} mol m^{-2} s^{-1} Pa^{-1} and ideal selectivities of 7.3, 15.5, 16.2, and 2655 for H_2/CO_2, H_2/N_2, H_2/CH_4, and H_2/C_3H_8, respectively, were achieved. Also, an ultrahigh C_3H_6 permeance of

Dr. G. He, M. Dakhchoune, J. Zhao, S. Huang, Prof. K. V. Agrawal
Laboratory of Advanced Separations (LAS)
École Polytechnique Fédérale de Lausanne (EPFL)
CH-1951 Sion, Switzerland
E-mail: kumar.agrawal@epfl.ch

The ORCID identification number(s) for the author(s) of this article can be found under https://doi.org/10.1002/adfm.201707427.

**ADVANCED
SCIENCE NEWS**
www.advancedsciencenews.com

**ADVANCED
FUNCTIONAL
MATERIALS**
www.afm-journal.de

Figure 1. Schematic illustration of the ENACT process for the synthesis of MOF films on a variety of substrates.

9.9×10^{-8} mol m^{-2} s^{-1} Pa^{-1} and an attractive C$_3$H$_6$/C$_3$H$_8$ selectivity of 31.6 were obtained. This was achieved by a novel electrophoretic nuclei assembly for crystallization of highly intergrown thin-films (ENACT) route that ensured a high density of heterogeneous nucleation on a wide range of unmodified substrates (ceramic, polymer, metal, sp^3-carbon, and graphene). The ENACT method is highly generic. As an extension of this method, we also report synthesis of 2.7 µm thick ZIF-7 film on the unmodified AAO support.

The ENACT approach utilizes electrophoretic deposition[23,24] of MOF nuclei onto a substrate under an external direct current electric field, directly from the precursor sol. Further growth of the MOF nuclei in the same precursor sol results in a highly intergrown MOF film. The application of an electric field to the charged nuclei mobilizes them toward an electrode with a flux that is proportional to the strength of applied electric field (E), electrophoretic mobility of colloid (μ), and concentration of nuclei (C_n) as per Equations (1) and (2)

$$\text{Nuclei Flux} \propto E\mu C_n \tag{1}$$

$$\mu = \frac{v}{E} = \frac{\varepsilon_o \varepsilon_r \zeta}{\eta} \tag{2}$$

where v is the drift velocity, ζ is the zeta potential of the colloid, ε_o is permittivity of vacuum, and ε_r and η are the dielectric constant and viscosity of the dispersing medium, respectively. Therefore, by controlling E and solution pH (which determines ζ of ZIF nuclei), one can control the heterogeneous nucleation density. As such, by controlling E, a highly packed nuclei layer can be formed even from a very dilute precursor sol. We note that although the electrophoretic deposition of crystals (including MOFs) on various conductive substrates has been demonstrated by several groups,[24,25] this is the first report on the synthesis of continuous highly intergrown, ultrathin MOF films on both conductive and nonconductive substrates using electrophoretic assembly (refer to Section III, Supporting Information).

2. Results and Discussion

### 2.1. Preparation of Nuclei Films

The ENACT method is demonstrated for ZIF-8 and ZIF-7 films considering their excellent thermal and chemical stability,

and molecular sieving properties for several industrially relevant gases.[26] **Figure 1** illustrates the heterogeneous nucleation of ZIF-8 on a porous support, and subsequent intergrowth of nuclei into a continuous film. Briefly, two separate aqueous solutions, 0.00926 mmol mL^{-1} of Zn(NO$_3$)$_2$·6H$_2$O and 0.691 mmol mL^{-1} of 2-methylimidazole, were prepared.[27] After mixing the two solutions for 3 min, a constant E of 100 V m^{-1} was applied between the electrodes, for up to 4 min. Under these conditions, the solution pH was 9.4, imparting a net positive surface charge to the ZIF-8 nuclei (ζ = 18.2 mV, Figure S1, Supporting Information). Driven by the electric field, the ZIF-8 nuclei assembled on the desired substrate positioned on the cathode. Investigation of the nuclei film on an AAO substrate revealed densely packed and crystalline ZIF-8 nuclei without large gaps or cracks (**Figure 2**a–c; Figure S2, Supporting Information).

2.2. ENACT Insights and Optimization

The ZIF-8 nuclei were crystallized at room temperature using the aqueous growth sol reported by Lai and co-workers.[19,28] Use of an aqueous growth sol provides a low-cost and environment-friendly route toward the potential scale-up of the membrane. However, nucleation and growth of the ZIF-8 crystals in this growth sol, especially at short times, have not been studied in detail. We used transmission electron microscopy (TEM) and electron diffraction (ED) to study formation of nuclei from the sol. Crystalline nonfaceted nanoparticles were present in the sol even at 60 s, indicating an induction time smaller than 60 s (Figure 2e–h; Figure S3, Supporting Information). The ED patterns are consistent with that of the ZIF-8 crystals.[28] ZIF-8 crystals evolve from 10.2 ± 2.4 (1 min of ageing) to 21.1 ± 5.1 nm (7 min of ageing) with average growth rates of 10.2 (0–1 min), 3.4 (1–3 min), 1.2 (3–5 min), and 0.9 nm min^{-1} (5–7 min), respectively (Figure 2d). The remarkable decrease in growth rate during the initial 7 min indicates a relatively high nucleation density in which the large nuclei population rapidly depleted the growth precursors.

To gain further insights into the induction of ZIF-8 and assembly of ZIF-8 nuclei, the morphology and crystallinity of the nuclei film deposited after 1–7 min of ageing were investigated. For this, ZIF-8 nuclei were rapidly collected on an
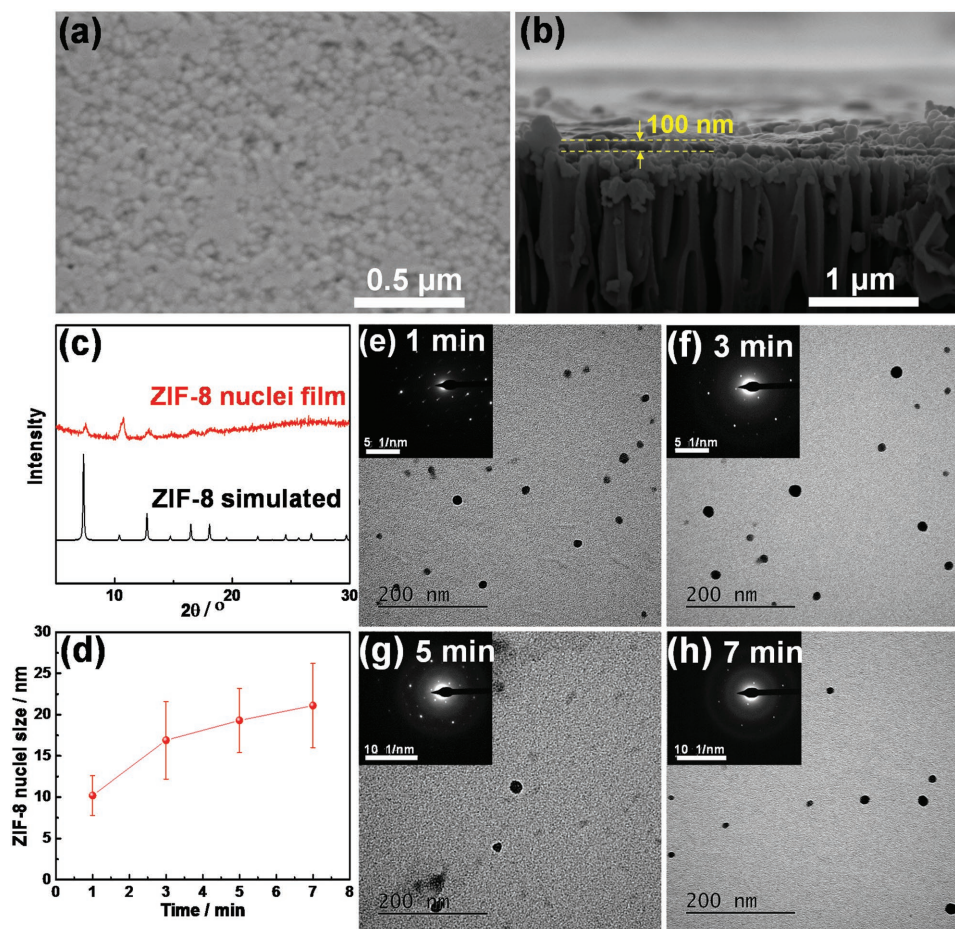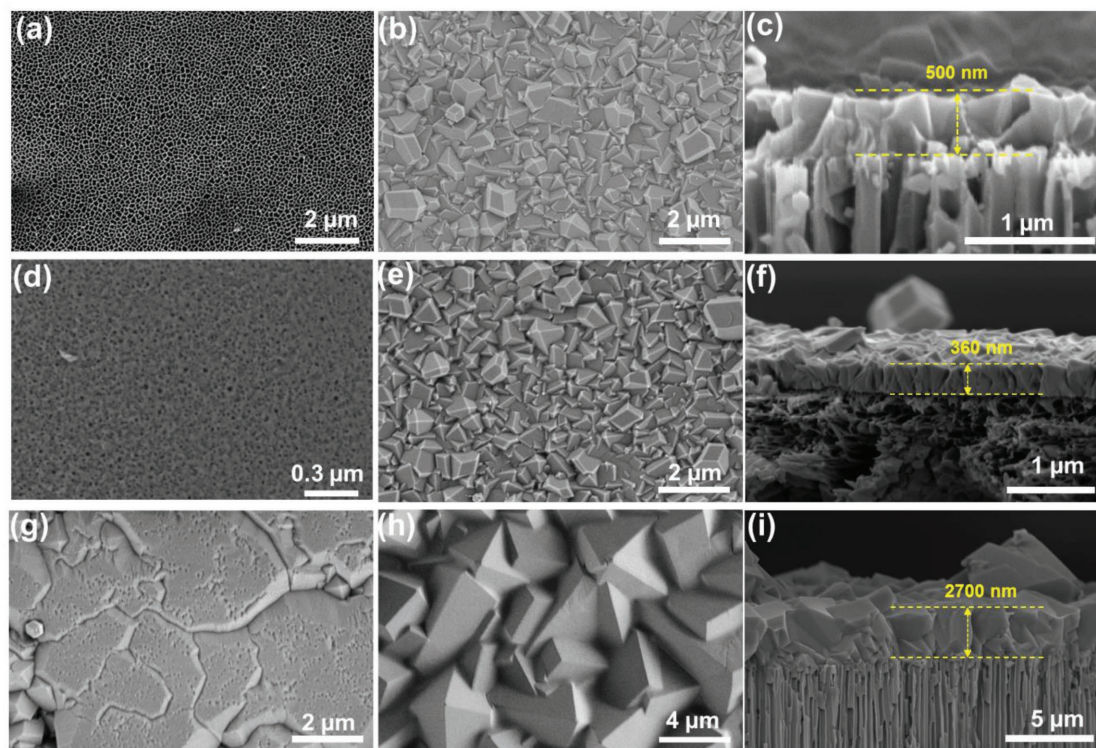
Figure 2. a) SEM image of ZIF-8 nuclei on AAO support, and b) the corresponding cross-sectional morphology. c) XRD patterns of simulated ZIF-8 crystal and the nuclei film on AAO. d) Average nuclei size at various ageing times. e–h) TEM images and ED patterns of ZIF-8 nuclei aged for various times.

indium tin oxide (ITO)-coated glass plate ($E = 1000$ V m^{-1}). The morphology of the film deposited at 1 min appears to be smooth attributing to the minuscule nuclei size, while the films deposited at 3–7 min reveal more granular morphologies (Figure S4, Supporting Information). In all cases, the nuclei films appear to be dense and uniform (Figure S4, Supporting Information). X-ray diffraction (XRD) patterns of the films confirm that the deposited nuclei are indeed ZIF-8, and that the induction time of ZIF-8 in this aqueous sol is shorter than 1 min (Figure S5, Supporting Information).

The ENACT process allows the deposition of highly packed nuclei directly from the synthesis sol within the timescale of a few minutes. The high density of nuclei film can then facilitate highly packed intergrown crystal grains in the same precursor sol. A close analogue to this is the seeding technique in which crystals are deposited on the support followed by secondary growth. However, this often involves several steps, including crystallization of seeds, purification of seeds from the precursor sol (by centrifugation, filtration, etc.), stabilization of seeds in a dispersing medium to formulate a coating suspension, coating of seeds, drying of the dispersing medium, etc.[29]

We were able to assemble ZIF-8 nuclei on nonconducting substrates (ceramic, polymer) by positioning the substrates directly on the cathode. The support pore opening was taken into consideration to optimize the sol ageing time. For example, it was difficult to deposit uniform nuclei film on AAO supports with a pore opening of 100 nm when the ageing time was less than 3 min (Figure S6, Supporting Information). In this case, the smaller nuclei did not fully cover the substrate pores. Some nuclei can be observed sitting at the top of the substrate wall. On the other hand, when the sol ageing time is longer than 3 min, a uniform nuclei film was achieved (Figure 2a). The nuclei film was ≈100 nm thick (Figure 2b). A minuscule fraction of ZIF-8 nuclei penetrated into the pores of AAO (Figure 2b; Figure S2d, Supporting Information).

To prove the effectiveness of the ENACT process compared with the conventional evaporation-induced self-assembly (EISA) method such as dip coating, we conducted a dip-coating experiment as a control. An AAO substrate soaked in the precursor sol during the 3–7 min of sol ageing was withdrawn at 0.1 cm s^{-1} to entrain the sol. Subsequent drying of the film revealed a surface that was sparingly coated with a coverage of less than 10% (Figure S7, Supporting Information). This can be

**ADVANCED
SCIENCE NEWS**
www.advancedsciencenews.com

**ADVANCED
FUNCTIONAL
MATERIALS**
www.afm-journal.de

Figure 3. Surface/cross-sectional morphologies of a) AAO support, b,c) ZIF-8/AAO membrane, d) PAN support, e,f) ZIF-8/PAN membrane, g) ZIF-8/graphene, and h,i) ZIF-7/AAO membrane.

attributed to the fact that the concentration of ZIF-8 nuclei in the synthesis sol was too low to enable successful EISA-based coatings.

2.3. Growth of ZIF-8 Membrane

ENACT approach is simple and straightforward to synthesize thin, intergrown MOF films. One could synthesize an intergrown MOF film by simply leaving the nuclei film in the synthesis sol for a short period of time. By leaving the nuclei film in the synthesis sol at 30 °C, the nuclei film grew continuously with average grain size increasing from 176 ± 105 nm at 2 h to 375 ± 93 nm at 8 h (Figure S8, Supporting Information). The packing of ZIF-8 grains increased with the increase of growth time, thus reducing pinhole defects. Increasing the growth time to 10 h led to highly intergrown ZIF-8 grains with an average grain size of 478 ± 174 nm (**Figure 3**). We did not detect any pinholes in the entire film, and the film had a uniform morphology (Figure S9, Supporting Information). The XRD pattern of the film matches well with that of the simulated ZIF-8 (**Figure 4**a), indicating that as-synthesized ZIF-8 film is comprised of the pure ZIF-8 phase. Thickness of this film was ≈500 nm (Figure 3c; Figure S10, Supporting Information), making it one of the thinnest intergrown MOF film synthesized without any substrate modification steps. As a control experiment, we performed secondary growth of the nuclei film, which was prepared by the dip coating in the precursor sol, for 10 h. The resulting film is comprised of numerous pinholes and

consequently not adequate as a membrane (Figure S11, Supporting Information). This comparison highlights the significant importance of the high-density nuclei facilitated by the ENACT approach.

2.4. Generality of the ENACT Approach

Synthesis of highly intergrown MOF films on low-cost porous polymer substrates is industrially attractive. It is noteworthy that unlike mixed matrix membranes, where MOF crystals are dispersed in the polymeric media, thin films of MOFs on porous polymeric supports yields higher selectivity and orders of magnitude higher permeance.[30] We selected a commercially available and widely used PAN membrane (pore size: 25 nm, Figure 3d) as a substrate for membrane fabrication. ZIF-8 membrane was crystallized on PAN support using the same protocol as described above. The resulting ZIF-8 film on PAN was well intergrown without pinholes, similar to the morphology of the membrane on AAO (Figure 3d; Figure S13a, Supporting Information). The film on the PAN support was crystalline (XRD pattern, Figure 4a), with XRD peaks corresponding to that of the lattice planes of ZIF-8. The cross-sectional imaging of this membrane revealed a film thickness of 360 nm (Figure 3f; Figure S13b, Supporting Information), making it one of the thinnest MOF membranes on polymer substrates.[31]

Apart from the porous ceramic and polymer substrates, we were successful in crystallizing highly intergrown ZIF-8 films (0.7–1.5 µm) on Cu foil, nanoporous
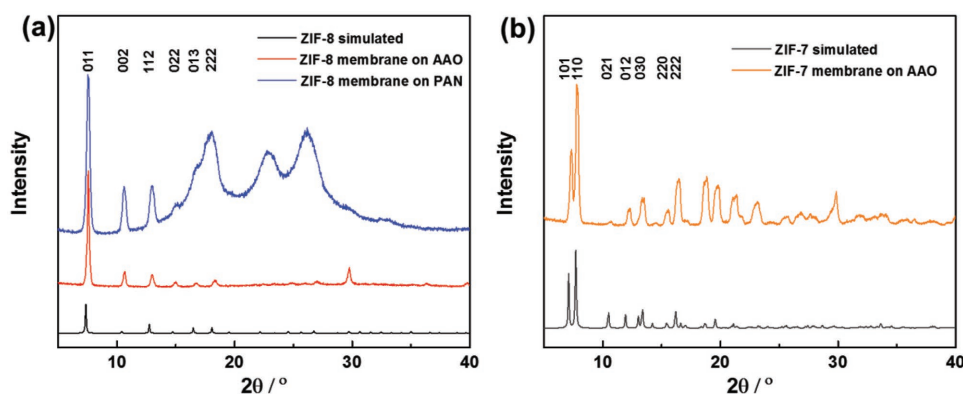
Figure 4. XRD patterns of a) ZIF-8 membranes on the AAO and the PAN support, and b) ZIF-7 film on the AAO support. The three wide peaks between 17° and 27° in the pattern of ZIF-8 membrane on PAN are the characteristic peaks of the PAN support (Figure S12, Supporting Information).

carbon, and graphene, which proves the applicability of the ENACT process to a broad range of substrates and potential applications such as sensors and microelectronics[32] (Figures S14–S17, Supporting Information). Interestingly, the ZIF-8 film on graphene is comprised of several seemingly oriented, 5–10 µm large ZIF-8 grains (Figure 3g; Figure S17b,c, Supporting Information), indicating a higher tendency of the oriented growth of ZIF-8 crystals on graphene. Such growth behavior can have important implications for fabricating high-performance MOF membranes, and will be investigated in detail in the future. While preparing scanning electron micrograph (SEM) samples for imaging the cross-sections of the ZIF-8 films, the films on Cu and graphene substrates delaminated, while the films on the AAO or PAN adhered to the porous supports even after intentionally cracking the membranes. This indicates that the membranes on AAO and PAN were mechanically robust. This can be attributed to the fact that the nuclei layer enters the pore-mouth of the porous supports, increasing the interfacial interactions via an anchoring effect.

The ENACT approach was successfully adapted for synthesis of a thin ZIF-7 film. For this, an AAO support was dipped in a ZIF-7 growth sol. After ageing the sol for 3 min, ZIF-7 nuclei were assembled into a dense film at 100 V m^{-1} for 1 min (Figure S18a,b, Supporting Information). A highly intergrown ZIF-7 film with a thickness of 2.7 µm was obtained by soaking the ZIF-7 nuclei film in the synthesis sol at 110 °C for 4 h (Figure 3h,i; Figure S18c,d, Supporting Information). The XRD pattern reveals that the ZIF-7 film was highly crystalline (Figure 4b). In contrast, using the dip-coating technique, Kim and Lee reported a much thicker (6.3 µm) ZIF-7 film.[33] This highlights the remarkable potential of the ENACT method in the crystallization of MOF thin films, attributing to the dense heterogeneous nucleation even from the dilute growth sols.
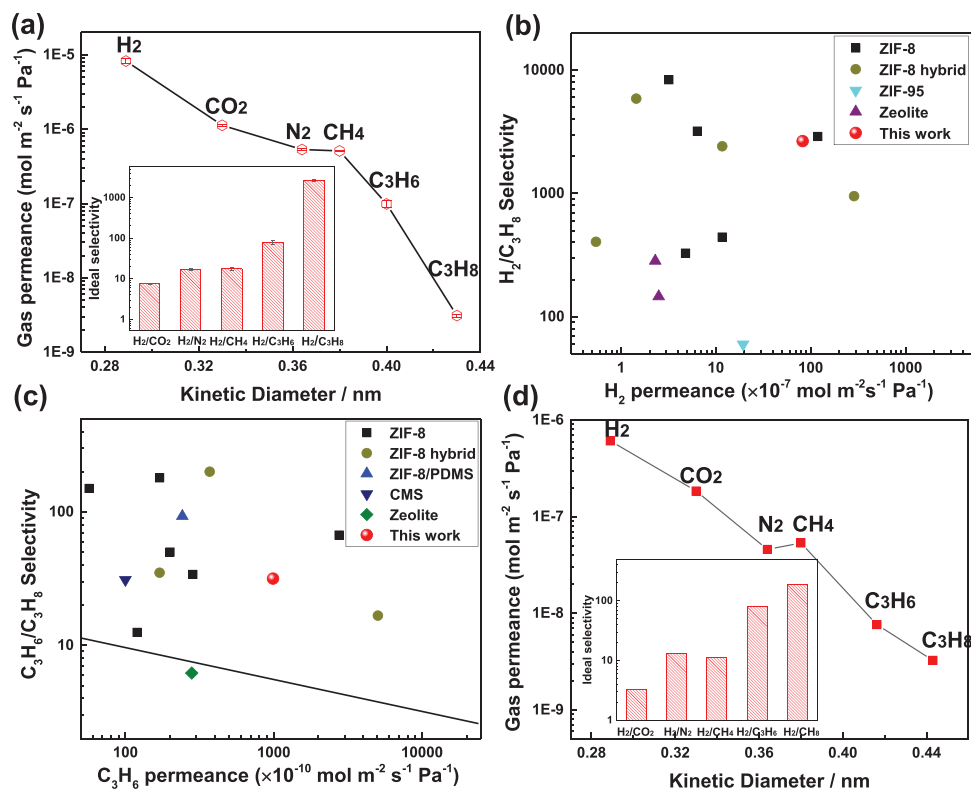
2.5. Gas Separation Performance of the ZIF-8 Membranes

The single-gas permeation results for H_2, CO_2, N_2, CH_4, C_3H_6, and C_3H_8 from ZIF-8 membranes on AAO are shown in **Figure 5**a. The ZIF-8 membrane exhibited a remarkably high H_2 permeance of 8.3×10^{-6} mol m^{-2} s^{-1} Pa^{-1}. Although ZIF-8 has a pore aperture of 0.34 nm, the flexibility of ZIF-8's nanoporous structure[34] allows molecules with kinetic diameters larger than 0.34 nm to diffuse through the ZIF-8 pores, albeit with a lower diffusivity. The ideal selectivities of H_2 with respect to CO_2, N_2, CH_4, C_3H_6, and C_3H_8 were 7.3 ± 0.3, 15.5 ± 1.4, 16.2 ± 1.4, 83.9 ± 7.4, and 2655.3 ± 131.0, respectively, far exceeding the corresponding Knudsen selectivities,[15,35] indicating a low defect density in the ZIF-8 films (Section IV, Supporting Information). These selectivities are comparable to the high-quality ZIF-8 membranes in the literature (Table S1, Supporting Information). In fact, ENACT-based ZIF-8 membranes exhibit one of the highest H_2 permeances among state-of-the-art MOF membranes. The high H_2 permeance combined with the high gas selectivity represents one of the best performances among MOF membranes (Figure 5b; Table S1, Supporting Information). This remarkable performance is mainly due to the ultrathin selective layer (500 nm) and a high degree of intergrowth of ZIF-8 grains. Moreover, the as-synthesized ZIF-8 membranes are highly reproducible (Table S2, Supporting Information). All five membranes made by the ENACT process yield similar gas separation performance.

We also studied separation of propylene from propane using the as-synthesized ZIF-8 membranes. The separation of propylene from propane is challenging because they possess similar physical properties. Currently, this separation is carried out by energy-intensive cryogenic distillation, and a sustainable energy-efficient separation process is greatly desired.[37,38] The diffusivity of C_3H_8 in ZIF-8 is two orders of magnitude smaller than that of C_3H_6 attributing to the small difference in their kinetic diameters; and therefore, the ZIF-8 membranes are promising for propylene/propane separation.[18,34] For instance, the Jeong group reported the synthesis of 300–400 nm thick ZIF-8 membranes via an Ostwald-ripening-like process, which yielded C_3H_6/C_3H_8 separation factor of 120 with C_3H_6 permeance of 1.3×10^{-8} mol m^{-2} s^{-1} Pa^{-1}.[39] The AAO-supported ZIF-8 membranes in this work exhibit an ideal selectivity of 31.6 for propylene/propane with a relatively high C_3H_6 permeance reaching 9.9×10^{-8} mol m^{-2} s^{-1} Pa^{-1} at 25 °C. The superior performance of our membrane with respect to those in the literature is clearly apparent in the Robeson like plot of propane/propylene selectivity versus gas permeance (Figure 5c).

Figure 5d shows the single-gas permeation properties of the ZIF-8/PAN membrane. The membrane exhibits a high H_2

**ADVANCED
SCIENCE NEWS**

www.advancedsciencenews.com

**ADVANCED
FUNCTIONAL
MATERIALS**

www.afm-journal.de

Figure 5. a) Permeances and ideal selectivities as a function of the kinetic diameters from the ZIF-8/AAO membrane at 25 °C and 1 bar. b) Comparison of H_2/C_3H_8 separation performance with the state-of-the-art membranes (Tables S1, S3, and S4, Supporting Information). c) Comparison of propylene/propane separation performance with the state-of-the-art membranes (Table S3, Supporting Information). The black line represents the propylene/propane upper bound for single-gas permeances from polymeric membranes.[36] d) Permeances and ideal selectivities of various gases as a function of their kinetic diameters from the ZIF-8/PAN membrane at 25 °C and 1 bar.

permeance of 6.1×10^{-7} mol m^{-2} s^{-1} Pa^{-1} and ideal selectivities of 3.3, 13.3, 11.4, 79.0, and 187 with respect to CO_2, N_2, CH_4, C_3H_6, and C_3H_8, respectively. H_2 permeance from the ZIF-8/PAN membrane is much lower than that from the ZIF-8/AAO membrane because of the significantly higher gas-transport resistance from the PAN support compared with that from the AAO support.[16] Nevertheless, the separation performance of the ZIF-8/PAN membrane is still highly attractive. A comprehensive comparison with state-of-the-art MOF membranes is provided in Tables S1, S3, and S4 in the Supporting Information.

3. Conclusion

In summary, we have developed a facile ENACT approach enabling the synthesis of highly permselective, ultrathin MOF films on a wide range of porous and nonporous substrates (ceramic, polymer, metal, nanoporous carbon, and graphene). The ENACT approach allows an effective control of nuclei size and heterogeneous nucleation density over a substrate, facilitating a high degree of grain intergrowth while minimizing the film thickness. Notably, any substrate pretreatment is completely avoided, making this approach quite attractive for the synthesis of MOF membranes. As a result, a high H_2 permeance of 8.3×10^{-6} mol m^{-2} s^{-1} Pa^{-1} and ideal gas selectivities of 7.3, 15.5,

16.2, 2655, and 31.6 were achieved for H_2/CO_2, H_2/N_2, H_2/CH_4, H_2/C_3H_8, and C_3H_6/C_3H_8 gas pairs, respectively, from 500 nm thick ZIF-8 films, making these membranes as one of the best performing gas separation membranes. The ENACT approach is versatile, straightforward, highly reproducible and can be extended to a wide range of nanoporous crystals.

4. Experimental Section

Preparation of Substrates: AAO supports (diameter: 13 mm, pore size: 100 nm) were obtained from GE Healthcare. PAN membranes with a molecular weight cut-off of 100 kDa were obtained from Shandong MegaVision Membrane Technology & Engineering Co. Ltd. Cu foil was obtained from Alfa Aesar. Before nuclei assembly, the AAO support and the Cu foil were rinsed with water and isopropanol, and the PAN support was rinsed with water. The graphene film on a Cu foil was synthesized as reported elsewhere.[40] Nanoporous carbon film was synthesized by a method reported by Fan and co-workers.[41]

Preparation of ZIF-8 Film: First, an aqueous solution (60 mL) containing 0.00926 mmol mL^{-1} of Zn(NO$_3$)$_2$.6H$_2$O and 0.691 mmol mL^{-1} of Hmin was prepared. After stirring the precursor sol for 30 s, two parallel Cu electrodes separated by 1 cm were positioned into the solution, with a substrate (AAO, PAN, nanoporous carbon, and graphene) mounted on the top of the cathode. Then, after ageing the precursor sol for 1–3 min, an electric field was applied (100 V m^{-1}) for up to 4 min. The ZIF-8 nuclei film on ITO was prepared by applying a

**ADVANCED
SCIENCE NEWS**

www.advancedsciencenews.com

**ADVANCED
FUNCTIONAL
MATERIALS**

www.afm-journal.de

higher electric field, 1000 V m^{-1}, for 10 s, followed by flash drying of the coated film in a nitrogen flow to terminate the crystal growth. By this way, a thick nuclei film from solution aged for a specific time (1, 3, 5, or 7 min) was deposited on the ITO for characterization by XRD. To synthesize an intergrown film, the nuclei film was left soaking in the precursor sol at 30 °C for 10 h. Finally, the ZIF-8 film was thoroughly rinsed with water and dried at room temperature.

Preparation of ZIF-7 Film: The ZIF-7 film on an AAO substrate was prepared by the similar method used for the ZIF-8 films but with the following differences. The precursor sol was prepared by mixing 0.816 g Zn(NO$_3$)$_2$·6H$_2$O in 30 mL dimethylformamide (DMF) and 0.72 g benzimidazole in 30 mL methanol.[33] After ageing the sol for 3 min, the nuclei assembly was carried out for 1 min. An intergrown ZIF-7 film was crystallized by soaking the ZIF-7 nuclei film in a precursor sol containing 0.58 g Zn(NO$_3$)$_2$·6H$_2$O, 0.3 g benzimidazole, and 30 mL DMF at 110 °C for 4 h.[33] After cooling the solution, the ZIF-7 film was washed by DMF followed by drying at 60 °C for 12 h.

Characterization: The morphologies of MOF films were observed using the FEI Teneo SEM. The surface morphology of nanoporous carbon was observed using the Zeiss MERLIN SEM. The nuclei size and crystallinity was studied using FEI Tecnai G2 Spirit TEM. The ZIF-8 at *X* min (*X* represents the ageing time) nuclei samples were prepared by diluted the precursor sol by 100 times (for *X* = 1 min) or 200 times (for *X* = 3, 5, and 7 min), followed by depositing the solution on a TEM grid, and subsequently flash drying the TEM grid in nitrogen flow to terminate crystal growth. XRD was conducted using a Bruker D8 Discover X-ray diffractometer equipped with a laser alignment system. ζ measurement was performed using Zetasizer Nano ZS (Malvern Instruments, UK).

Single-gas permeances were measured by the Wicke–Kallenbach technique using a homemade permeation setup (Figure S19, Supporting Information).[19] The pressure on the feed and the permeate side were maintained at 1 bar. Argon was used as the sweep gas. The membranes were sealed on an annular stainless steel disk by epoxy. The permeate compositions were analyzed by a mass spectrometer (Hiden Analytical, HPR-20). All measurements were performed after reaching the steady-state condition. To remove the adsorbed water during the synthesis, the ZIF-8/AAO membranes were dried at 130 °C under a H$_2$/Ar atmosphere until a steady H$_2$ permeance was reached. The ZIF-8/PAN membranes were first rinsed in methanol, followed by soaking in methanol for 30 min to exchange the water. Subsequently, the drying was performed at 60 °C until a steady H$_2$ permeance was reached. The permeances, J_i, of the gas *i* were calculated by Equation (3)

$$J_i = X_i/(A \cdot \Delta P_i) \tag{3}$$

where X_i is the flow rate of gas *i*, A the membrane area, and ΔP_i is the transmembrane pressure difference of species *i*. The ideal selectivity α_{ij} of the two gases (*i* and *j*, where *i* is the faster permeating gas) was calculated by Equation (4)

$$\alpha_{ij} = \left(C_i/C_j\right)_{permeate}/\left(C_i/C_j\right)_{feed} \tag{4}$$

where C_i is the concentration of gas species *i* in a given stream.

Supporting Information

Supporting Information is available from the Wiley Online Library or from the author.

Acknowledgements

Conflict of Interest

The authors declare no conflict of interest.

Keywords

[1] A. Knebel, B. Geppert, K. Volgmann, D. I. Kolokolov, A. G. Stepanov, J. Twiefel, P. Heitjans, D. Volkmer, J. Caro, *Science* **2017**, *358*, 347.

[2] A. J. Brown, N. A. Brunelli, K. Eum, F. Rashidi, J. R. Johnson, W. J. Koros, C. W. Jones, S. Nair, *Science* **2014**, *345*, 72.

[3] O. Shekhah, J. Liu, R. A. Fischer, C. Wöll, *Chem. Soc. Rev.* **2011**, *40*, 1081.

[4] S. Couck, J. F. M. Denayer, G. V Baron, T. Rémy, J. Gascon, F. Kapteijn, *J. Am. Chem. Soc.* **2009**, *131*, 6326.

[5] A. L. Dzubak, L.-C. Lin, J. Kim, J. A. Swisher, R. Poloni, S. N. Maximoff, B. Smit, L. Gagliardi, *Nat. Chem.* **2012**, *4*, 810.

[6] Y. Li, F. Liang, H. Bux, A. Feldhoff, W. Yang, J. Caro, *Angew. Chem., Int. Ed.* **2010**, *122*, 558.

[7] Y. Hu, X. Dong, J. Nan, W. Jin, X. Ren, N. Xu, Y. M. Lee, *Chem. Commun.* **2011**, *47*, 737.

[8] J. Gascon, F. Kapteijn, *Angew. Chem., Int. Ed.* **2010**, *49*, 1530.

[9] X. Liu, C. Wang, B. Wang, K. Li, *Adv. Funct. Mater.* **2017**, *27*, 1.

[10] N. Rangnekar, N. Mittal, B. Elyassi, J. Caro, M. Tsapatsis, *Chem. Soc. Rev.* **2015**, *44*, 7128.

[11] Y. Peng, Y. Li, Y. Ban, H. Jin, W. Jiao, X. Liu, W. Yang, *Science* **2014**, *346*, 1356.

[12] Z. Wang, A. Knebel, S. Grosjean, D. Wagner, S. Bräse, C. Wöll, J. Caro, L. Heinke, *Nat. Commun.* **2016**, *7*, 13872.

[13] F. Zhang, X. Q. Zou, X. Gao, S. J. Fan, F. X. Sun, H. Ren, G. S. Zhu, *Adv. Funct. Mater.* **2012**, *22*, 3583.

[14] F. Cacho-Bailo, I. Matito-Martos, J. Perez-Carbajo, M. Etxeberría-Benavides, O. Karvan, V. Sebastián, S. Calero, C. Téllez, J. Coronas, *Chem. Sci.* **2017**, *8*, 325.

[15] A. Huang, Q. Liu, N. Wang, Y. Zhu, J. Caro, *J. Am. Chem. Soc.* **2014**, *136*, 14686.

[16] E. Barankova, X. Tan, L. F. Villalobos, E. Litwiller, K. V. Peinemann, *Angew. Chem., Int. Ed.* **2017**, *56*, 2965.

[17] K. Eum, A. Rownaghi, D. Choi, R. R. Bhave, C. W. Jones, S. Nair, *Adv. Funct. Mater.* **2016**, *26*, 5011.

[18] H. T. Kwon, H.-K. Jeong, *J. Am. Chem. Soc.* **2013**, *135*, 10763.

[19] Y. Pan, T. Li, G. Lestari, Z. Lai, *J. Membr. Sci.* **2012**, *390–391*, 93.

[20] J. Hou, P. D. Sutrisna, Y. Zhang, V. Chen, *Angew. Chem., Int. Ed.* **2016**, *55*, 3947.

[21] Y. Hu, J. Wei, Y. Liang, H. Zhang, X. Zhang, W. Shen, H. Wang, *Angew. Chem., Int. Ed.* **2016**, *55*, 2048.

[22] W. Li, P. Su, Z. Li, Z. Xu, F. Wang, H. Ou, J. Zhang, G. Zhang, E. Zeng, *Nat. Commun.* **2017**, *8*, 406.

[23] L. Besra, M. Liu, *Prog. Mater. Sci.* **2007**, *52*, 1.

[24] I. Hod, W. Bury, D. M. Karlin, P. Deria, C. W. Kung, M. J. Katz, M. So, B. Klahr, D. Jin, Y. W. Chung, T. W. Odom, O. K. Farha, J. T. Hupp, *Adv. Mater.* **2014**, *26*, 6295.

[25] H. Zhu, H. Liu, I. Zhitomirsky, S. Zhu, *Mater. Lett.* **2015**, *142*, 19.

[26] Y. Liu, Y. Ban, W. Yang, *Adv. Mater.* **2017**, *29*, 1606949.

[27] Y. Pan, Y. Liu, G. Zeng, L. Zhao, Z. Lai, *Chem. Commun.* **2011**, *47*, 2071.

[28] Y. Pan, Z. Lai, *Chem. Commun.* **2011**, *47*, 10275.

[29] J. Yao, H. Wang, *Chem. Soc. Rev.* **2014**, *43*, 4470.

[30] S. Wang, X. Li, H. Wu, Z. Tian, Q. Xin, G. He, D. Peng, S. Chen, Y. Yin, Z. Jiang, *Energy Environ. Sci.* **2016**, *9*, 1863.

[31] E. Shamsaei, Z.-X. Low, X. Lin, A. Mayahi, H. Liu, X. Zhang, J. Zhe Liu, H. Wang, *Chem. Commun.* **2015**, *51*, 11474.

[32] I. Stassen, M. Styles, G. Grenci, H. V. Gorp, W. Vanderlinden, S. D. Feyter, P. Falcaro, D. De Vos, P. Vereecken, R. Ameloot, *Nat. Mater.* **2015**, *15*, 304.

[33] J. Kim, D. Lee, *J. Mater. Chem. A* **2016**, *4*, 5205.

[34] K. Zhang, R. P. Lively, C. Zhang, R. R. Chance, W. J. Koros, D. S. Sholl, S. Nair, *J. Phys. Chem. Lett.* **2013**, *4*, 3618.

[35] E. Shamsaei, X. Lin, L. Wan, Y. Tong, H. Wang, *Chem. Commun.* **2016**, *52*, 13764.

[36] R. L. Burns, W. J. Koros, *J. Membr. Sci.* **2003**, *211*, 299.

[37] H. T. Kwon, H. K. Jeong, A. S. Lee, H. S. An, J. S. Lee, *J. Am. Chem. Soc.* **2015**, *137*, 12304.

[38] D. Liu, X. Ma, H. Xi, Y. S. Lin, *J. Membr. Sci.* **2014**, *451*, 85.

[39] H. T. Kwon, H.-K. Jeong, A. S. Lee, H. S. An, T. Lee, E. Jang, J. S. Lee, J. Choi, *Chem. Commun.* **2016**, *52*, 11669.

[40] X. Li, W. Cai, J. An, S. Kim, J. Nah, D. Yang, R. Piner, A. Velamakanni, I. Jung, E. Tutuc, *Science* **2009**, *324*, 1312.

[41] A. T. Rodriguez, X. Li, J. Wang, W. A. Steen, H. Fan, *Adv. Funct. Mater.* **2007**, *17*, 2710.